CRITICAL SPEED ANALYSIS OF AN EIGHT-STAGE CENTRIFUGAL PUMP

by

Kenneth E. Atkins

Project Engineer

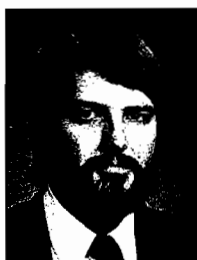**James D. Tison**

Senior Project Engineer

and

J. C. (Buddy) Wachel

Manager of Engineering

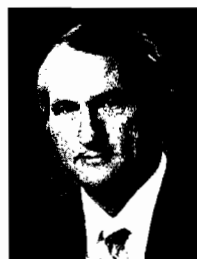Engineering Dynamics Incorporated

San Antonio, Texas

Kenneth E. Atkins is a Project Engineer with Engineering Dynamics, Incorporated, and has experience in performing lateral and torsional critical speeds, rotor stability analyses and the evaluation of structural vibration problems using finite element methods. He has been actively involved in field troubleshooting of a wide variety of rotordynamics, structural and piping vibrations. He has a B.S. degree in Engineering Science from Trinity University and is a registered professional engineer in the State of Texas.

James D. Tison is a Project Engineer with Engineering Dynamics, Incorporated. He is active in solving major industrial vibration problems in the power and petrochemical industries, utilizing field measurement and computer modeling techniques. He has developed and applied computer codes in the areas of torsional and lateral critical speeds, lateral instabilities, balancing, reciprocating equipment, crankshaft and frame loading and structural vibration. He has B.S. and M.E. degrees in Mechanical Engineering from the University of Florida. He is a member of ASME and Pi Tau Sigma.

J. C. (Buddy) Wachel is President of Engineering Dynamics, Incorporated, an independent engineering consulting firm. He has over 25 years of experience in the field of vibration analysis and has solved vibration problems worldwide. He has published over 30 technical papers in rotordynamics, piping vibrations and acoustics. He holds B.S. and M.S. degrees in Mechanical Engineering from the University of Texas. He is a member of ASME, PI Tau Sigma and Tau Beta Pi and is a registered professional engineer in the State of Texas.

ABSTRACT

A critical speed and unbalance response analysis of an eight-stage centrifugal pump was performed, considering the variation of stiffness and damping coefficients with speed for both the oil film bearings and the fluid seals (interstage, neck ring and balance piston). The rotor response to unbalance was predicted and compared to measured test stand data, utilizing four different methods to estimate the fluid seal effects. The comparison showed that correlation was best when using the latest finite length seal procedures. The wide variation in predicted critical speeds and response amplitudes indicates the need for additional research in this area, to define the exact stiffness and damping values for fluid film seals.

INTRODUCTION

The importance of analyzing the lateral critical speed of rotating equipment in the design stage is well known. The cost of downtime and maintenance caused by high lateral vibration in rotating equipment far exceeds the cost of a careful rotordynamic analysis. Although the state-of-the-art of lateral critical speed analysis has progressed greatly in the last few decades, the challenge of accurate simulation of pump rotor response and stability is the subject of a continuing research effort.

Pump rotordynamics are dependent on a greater number of design variables than are many other types of rotating equipment. Besides the journal bearing and shaft characteristics, the dynamic characteristics of the seals and the impeller-diffuser interaction can have significant effects on the critical speed location, rotor unbalance sensitivity, and rotor stability. Unfortunately, the accuracy of computations of stiffness and damping properties for seals and impeller effects is questionable even when all the state-of-the-art capabilities are included. The high pressure turbo-pumps of the space shuttle main engine are a prime example of the difficulty in accurately modelling seal effects [1].

For modelling purposes, seals can be treated as bearings in the sense that direct and cross-coupled stiffness and damping properties can be calculated based on the seal's hydrostatic and hydrodynamic properties. Seal clearances, geometry, pressure drop, fluid properties, inlet swirl, surface roughness and shaft speed are all important in these calculations. Since the pressure drop across seals increases approximately with the square of the pump speed, the seal stiffness also increases with the square of the speed. This increasing stiffness effect is often thought of as a "negative" mass effect, which is usually referred to as the "Lomakin effect" or the "Lomakin mass" [2]. In some cases the

theoretical Lomakin mass or stiffness effect can be of sufficient magnitude to prevent the critical speed of the rotor from ever being coincident with the synchronous speed.

Adequate experimental data exist today to document that the analytical procedures used for simulating the rotor response and stability of compressors and turbines are sufficiently accurate to predict critical speeds and potential instabilities from the design information. This analysis is not available for pumps, however—especially for pumps which use grooved seals, labyrinth seals, or screw type seals with several leads. The accurate prediction of the stiffness and damping properties of seals for different geometries and operating conditions is a subject of ongoing research [3,4,5]. The basic theories presented by Black [6] have been modified to account for finite length seals, inlet swirl, surface roughness, and other important parameters. However, a universally accepted procedure to accurately predict seal properties is not available for all the types of seals that are in use today. This is particularly true for grooved seals. If the seal effects are not correctly modelled, calculated critical speeds can be significantly different from actual critical speeds.

The rotordynamic analysis of an eight-stage centrifugal pump which utilized serrated (grooved) seals is discussed. Using the corrections for serrated seals as suggested by Black and Cochrane [7], the first critical speed was calculated to be above the running speed of 3550 rpm. When the shop acceptance tests were made on the pump, peak vibration responses occurring at as low as 1500 rpm were measured. The calculated critical speed of the pump varied from 1700 to 6000 rpm, depending upon which theory was used to develop the seal stiffness and damping coefficients. This example illustrates the need for additional research in this area.

CRITICAL SPEED ANALYSIS

Critical Speed Map—No Seal Effects

The first step in a rotordynamic analysis of a pump is to model the basic rotor, using the lumped parameter techniques. A sketch of the rotor with the location of the seals and bearings is given in Figure 1. Even though the bearings and seals add considerable cross-coupling and damping, the authors have found that it is still desirable to generate an undamped critical speed map to establish the range of the undamped (dry) critical speeds.
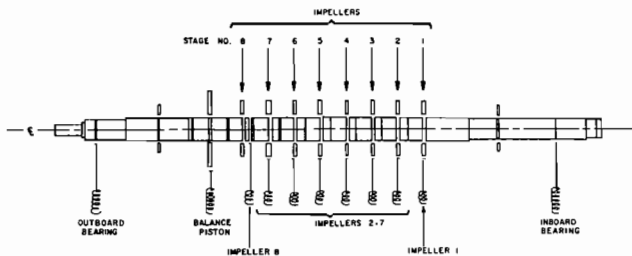

Figure 1. Pump Rotor Model Showing Locations of All Eleven Effective Bearings.

After the undamped critical speed map is developed, the bearings are analyzed to calculate the stiffness and damping characteristics over the entire speed range of operation. The bearing stiffness and damping characteristics can be simulated by using eight coefficients representing the direct and cross-coupled stiffness and damping terms for the specific values of oil viscosity, speed, diameter and length of bearing, clearance, and load (Sommerfeld number). Generally, bearing properties are calculated at small speed increments from the minimum to the maximum speed. These values are used when the forced

vibration response analysis is performed so that accurate predictions of the critical speeds can be obtained. Bearing characteristics that are assumed to be independent of speed should not be used, since this can result in incorrect predictions of the critical speeds. The major axis bearing stiffness curves (K_{xx} and K_{yy}) are usually plotted on the undamped critical speed map, so that the location of the pump critical speeds for no seals (or extremely worn seals) can be estimated. The journal bearings for the eight-stage pump were five-shoe load-between-pad pivotted shoe bearings. The assembled clearance range analyzed was five to eight mils diametrical for a preload value of 0.2.

The critical speed map for the "dry rotor" model, i.e., no supports considered at the seals, is shown in Figure 2. The first four undamped lateral critical speeds are plotted versus the bearing support stiffness. Horizontal and vertical journal bearing stiffness curves (K_{xx} and K_{yy}) for both the minimum and the maximum assembled clearances are also shown. Intersections between the bearing stiffness curves and the mode curves represent undamped critical speeds. These intersections are circled in Figure 2. Note that the "Mode 1" curve is fairly flat in the region where the intersections occur. The first two lateral mode shapes were then calculated for a nominal bearing stiffness of 500,000 lb/in and are shown in Figures 3 and 4.
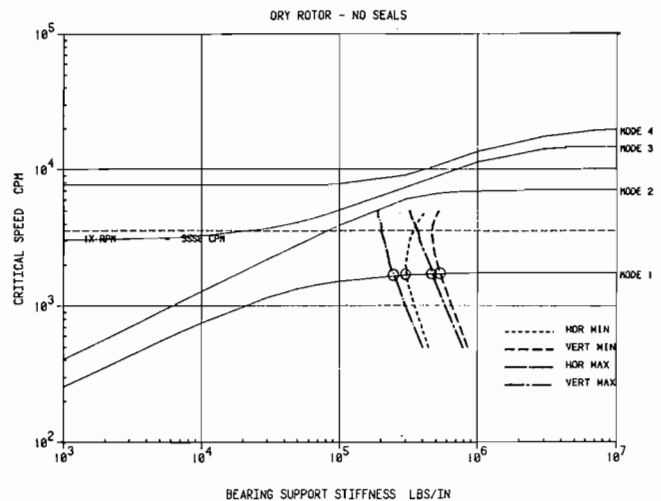

Figure 2. Lateral Critical Speed Map for No Seal Effects. Principal horizontal and vertical bearing stiffnesses for minimum and maximum bearing clearances are superimposed.

The dry rotor undamped natural frequencies as predicted by the critical speed map for the first, second, and third modes were 1710, 6650, and 8830 cpm, respectively.

Seal Effects

The forces in annular pressure seals can have a significant effect on the vibration characteristics of a pump rotor. The hydrodynamic and hydrostatic forces involved can significantly affect unbalanced response characteristics. The fluid film interaction with the shaft and the pressure drop across the seal give rise to a load capacity and a set of dynamic stiffness and damping coefficients similar to those used to represent the oil film in journal bearings. Black [6] presented the basic theory for short seals with smooth surfaces. For small motion about a centered position, the relation between the reaction-force components and shaft motion may be expressed as

$$\begin{Bmatrix} -F_x \\ -F_y \end{Bmatrix} = \begin{bmatrix} K & k \\ -k & K \end{bmatrix} \begin{Bmatrix} X \\ Y \end{Bmatrix} + \begin{bmatrix} C & c \\ -c & C \end{bmatrix} \begin{Bmatrix} \dot{X} \\ \dot{Y} \end{Bmatrix} + \begin{bmatrix} M & m \\ -m & M \end{bmatrix} \begin{Bmatrix} \ddot{X} \\ \ddot{Y} \end{Bmatrix}$$
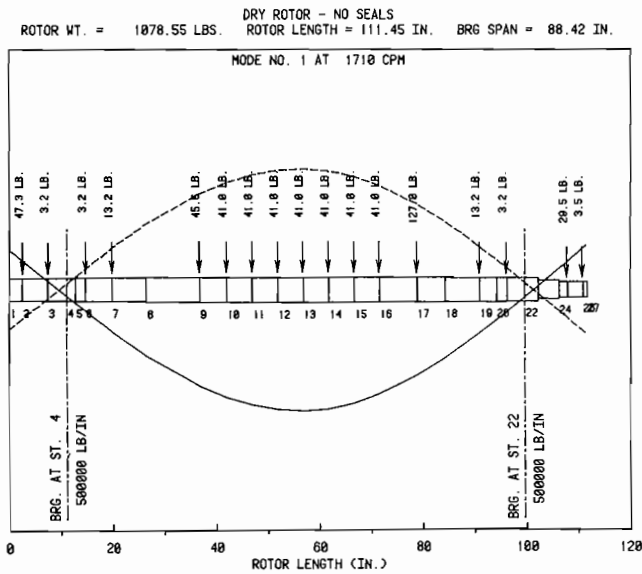
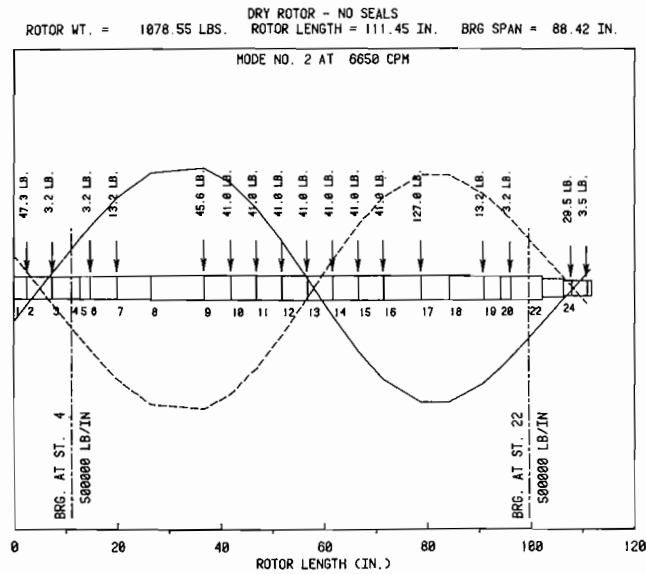*Figure 3. Mode Shape of First Lateral Critical Speed for No Seal Effects.*

Figure 4. Mode Shape of Second Lateral Critical Speed for No Seal Effects.

where (F_x, F_y) and (X,Y) are components of the reaction force and displacement vectors, respectively, and

K = direct stiffness
k = cross-coupled stiffness
C = direct damping
c = cross-coupled damping
M = direct added-mass coefficient
m = cross-coupled added-mass coefficient

Unlike hydrodynamic bearings, seals develop a significant amount of direct stiffness in the centered, zero-eccentricity position due to the distribution of the axial pressure drop between the inlet losses and an axial pressure gradient due to friction losses. The cross-coupled stiffnesses arise due to fluid rotation (swirl) within the seal. As a fluid element proceeds axially along an annular seal, shear forces at the rotor accelerate or decelerate the fluid tangentially until an asymptotic value is reached. For a seal with the same directionally homogeneous

surface-roughness treatment on the rotor and the housing, the average asymptotic tangential velocity is $R\omega/2$, where R is the seal radius and ω is the rotor running speed. The cross-coupled stiffness coefficient (k) acts in opposition to the direct damping coefficient (C) to destabilize rotors. Hence, steps which can be taken to reduce the net fluid rotation within a seal will improve rotor stability by reducing k [8].

Childs has defined the dynamic seal coefficients for plain short seals directly from Hirs' lubrication equations [3] and included the influence of the fluid inertia terms and inlet swirl. His assumptions were less restrictive than any previous derivation known to the authors. The derived coefficients are in reasonable agreement with prior results of Black and Jenssen [9].

Childs [4] then extended the analysis to include finite-length seals. This analysis included variable inlet swirl conditions (different from $R\omega/2$) and considered perturbations in the axial and circumferential Reynolds numbers due to a perturbation in clearances. Although more comprehensive, the results predicted negative cross-coupled stiffness coefficients for short seals (L/D<0.2).

A combined analytical-computational method has also been developed by Childs and Kim [5] to calculate the transient pressure field and dynamic coefficients for "damper seals" which use a rough stator and smooth rotor [10]. The solution procedure applies to constant-clearance or convergent-tapered geometries which may have different surface-roughness treatments of the stator or rotor seal elements. Analysis predictions have been compared to experimental results for several roughened stator designs, such as knurled-indentation, diamond-grid post pattern, and round-hole pattern. An extension of the analysis procedure due to Childs and Kim [5] is presently under development for either circumferentially or helically-grooved seals.

When grooved seals are used in a pump, a procedure must be found that can calculate the stiffness and damping values of the seals. At the present time, there are only a few techniques available in the open technical literature. Black and Cochrane [7] is probably the best known. Allaire, et al., have discussed this in their work [11]. Gopalakrishnan, et al., [2] gave simplified expressions for grooved seals in their paper on the effects of the Lomakin mass (or the Lomakin stiffness) on the critical speeds in pumps. Childs and Kim are presently performing tests to further investigate the theory that was discussed previously. Other techniques may exist; however, they are either proprietary or are not in general use.

The following procedures were used in determining the stiffness and damping values for the neck ring, interstage bushings and balance piston of the eight-stage pump analyzed.

Allaire—Method 1

Research performed at the University of Virginia has led to the development of a computer program [11] which uses the theoretical work by Black. The computer program calculates spring and damping coefficients for eccentric seals, as a function of fluid properties and seal geometry. Although the program is not designed for grooved seals, the suggestion has been made that approximate values could be determined by considering the grooved seals as a series of short plain seals. The pressure drop across the seal is divided by the number of lands. The stiffness and damping values for one land with the proportionate pressure drop are calculated. To obtain the results for the grooved seal, these numbers for one land are multiplied by the number of lands.

Black and Cochrane—Method 2

Black and Cochrane indicate that an equivalent length for the seal can be used in the correction factors for finite length

seals. The equivalent length for serrated seals is equal to the sum of the land lengths and equivalent groove lengths for grooves with a depth less than four times the radial clearance. This equivalent length was used with the computer program mentioned in Method 1.

Reduced Length Seal—Method 3

Another way in which the spring and damping stiffnesses can be calculated is to assume that the seal with grooves has the same characteristics as a seal with the length equal to the sum of the land lengths.

Childs and Kim Grooved Seal Program—Method 4

As discussed earlier, Childs and Kim are currently testing a series of grooved seal designs used in commercial pumps. They have developed a technique whereby the seal geometry can be specified and the characteristics calculated for specific assumptions with regard to inlet swirl, groove design, etc. Hopefully this research will lead to a procedure to calculate the characteristics of any type of grooved or serrated seal. The seal testing is still in progress and is partially supported by NASA and the Texas A&M University Turbomachinery Research Consortium. The authors requested that Childs and Kim calculate stiffness and damping values for the serrated seals used on the eight-stage pump discussed herein, using their procedures.

A summary of the results of the seal calculations using the various procedures is given in Table 1. The seal coefficients in the table are for rated speed and design clearance and are shown in Figure 5. This tended to support the conclusion that treating grooved seals as a series of plain short seals underpredicts the seal coefficients, at least relative to the other methods. Method 2 predicts the highest seal coefficients. Method 3 predicts somewhat lower coefficients than those of Method 2. Method 4 predicts higher coefficients for the interstage and neck ring seals than Method 2. Note that a negative principal stiffness (K) value is predicted for the balance piston.

Critical Speed Map—Considering Seals

A critical speed map including support stiffnesses at the seals was developed (Figure 6). The neck ring seals and the interstage bushings were combined at each impeller. For this analysis the pump rotor was analyzed as if it had eleven bearings (two tilting-pad bearings, a balance piston, and eight
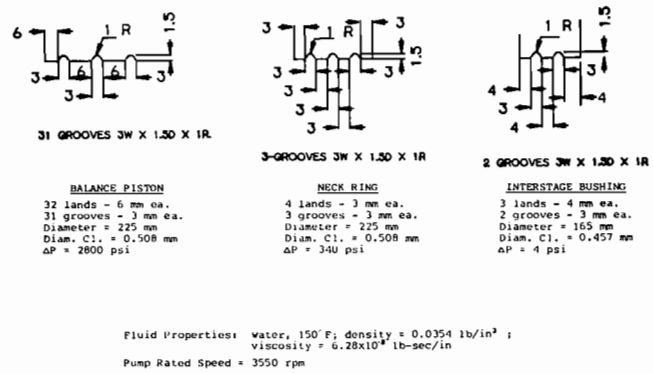

Figure 5. Neck Ring, Interstage Bushing and Balance Piston Seal Geometries with Fluid Properties and Seal Pressure Drops.
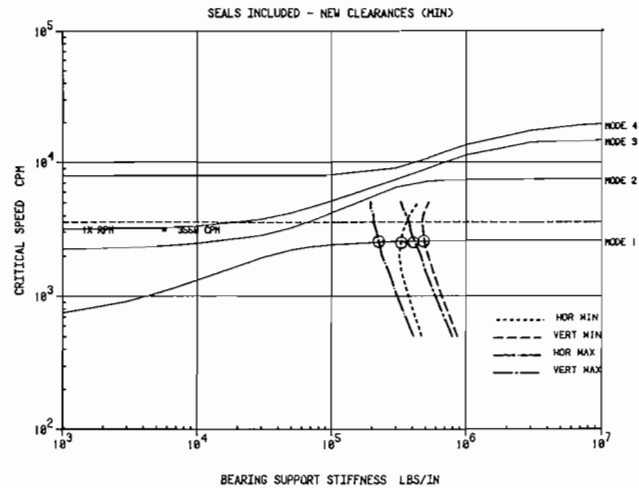

Figure 6. Lateral Critical Speed Map Including Effects of Minimum Clearance (New Seals). Principal horizontal and vertical bearing stiffnesses for minimum and maximum bearing clearances are superimposed.

seals located at the impellers) with the bearing stations as shown in Figure 1. For the purposes of this critical speed map analysis, the seal stiffness values were held constant at their maximum levels (minimum clearances which represent new seals) using Method 1.

Table 1. Summary of Seal Coefficients as Predicted by Various Methods.

| | | STIFFNESS | | DAMPING | |
| | | Principal k-lb/in | Cross Coupled k-lb/in | Principal c-lb sec/in | Cross Coupled c-lb sec/in |
Method	Seal Type				
1	Neck-Ring	3800	800	4	0
	Int-Stg Bush	40	150	1	0
	Balance Piston	102000	25000	140	3
2	Neck-Ring	48400	14800	80	0
	Int-Stg Bush	300	830	5	0
	Balance Piston	613000	332500	18000	3500
3	Neck-Ring	23700	5400	29	0
	Int-Stg Bush	200	400	2	0
	Balance Piston	912000	2000000	5600	600
4	Neck-Ring	13400	4900	23	0
	Int-Stg Bush	−8	370	3	0
	Balance Piston	−271000	627000	25000	3000

The lateral mode shape of the first critical speed including these seal effects (Method 1) is shown in Figure 7. A bearing stiffness value of 500,000 lb/in was again used for the mode shape calculations. Comparing Figure 7 with Figure 3, it is seen that the seals increase the frequency of the first mode without altering the mode shape significantly. For an assumed bearing stiffness of 500,000 lb/in, the first, second, and third critical speeds from Table 1 are 2570, 7120, and 8830 cpm, respectively.
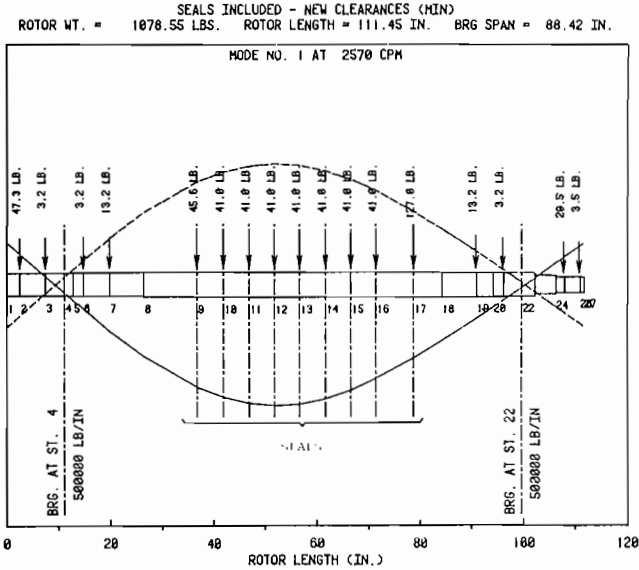

Figure 7. Mode Shape of First Lateral Critical Speed Including Seal Effects (New Seals).

Rotor Response to Unbalance

The location of a pump's critical speed is defined by its response to unbalance. It is important to recognize the difference between critical speeds excited by unbalance and damped eigenvalues which are sometimes also called critical speeds [12]. Generally, the effect of damping is to raise the frequency of the critical speed response due to unbalance; however, the effect of damping on the damped eigenvalues is to lower the frequency. The damped eigenvalues are primarily used for evaluating the stability of the rotor system. For compressors and turbines with tilting-pad bearings, the damped eigenvalues are usually comparable to the unbalanced response criticals. However, in a pump with a large number of seals, the added damping to the system can be considerable and there can be large differences in the unbalanced response critical speeds and the damped eigenvalues.

Rotor unbalance response calculations are the key analysis in the design stage for determining if a rotor is acceptable from a dynamics standpoint. As pointed out in [13], calculation of rotor unbalance response can be useless or largely incomplete if certain variables, such as unbalance location, bearing clearance, bearing preload, fluid properties, etc., are not properly considered.

The situation is further complicated when seal effects must be considered, as with centrifugal pumps. In order to bracket the expected range of critical speeds, the unbalance response of the eight-stage pump was analyzed with no seal effects and maximum bearing clearances, and with minimum seal and bearing clearances. The maximum bearing clearances/no seal case represents the overall minimum expected support stiffness for the rotor (lowest critical speed). The minimum clearance case represents the maximum expected support stiffness and, therefore, the highest critical speed. An intermediate case was

also considered with maximum bearing clearances and seal clearances of twice the design clearance to simulate worn seals. These parametric runs were made with seal characteristics calculated based on Method 1 described above.

The minimum calculated critical speed was 1700 cpm, as shown in Figure 8. This is the predicted unbalance response at the outboard bearing for the maximum bearing clearance, no seal effects case. The American Petroleum Institute (API) Standard 610 allowable unbalance was applied at the rotor midspan to excite the first mode. The results of the intermediate (worn seals) case are presented in Figure 9. The worn seals increase the predicted response peak to approximately 1800 cpm. With minimum clearances at the bearings and seals, the frequency increases to 2200 cpm, as shown in Figure 10.
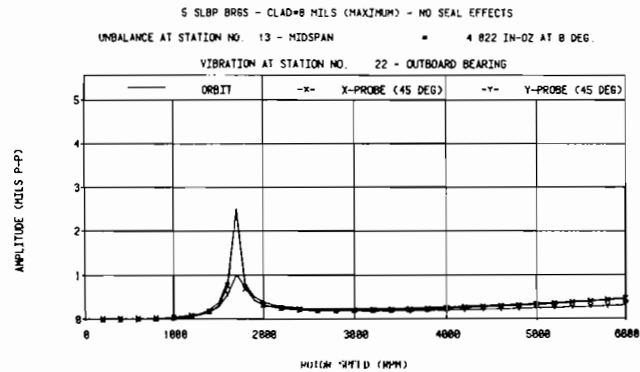

Figure 8. Calculated Unbalance Response at Outboard Bearing for API Unbalance at Midspan (No Seal Effects, Maximum Bearing Clearance).
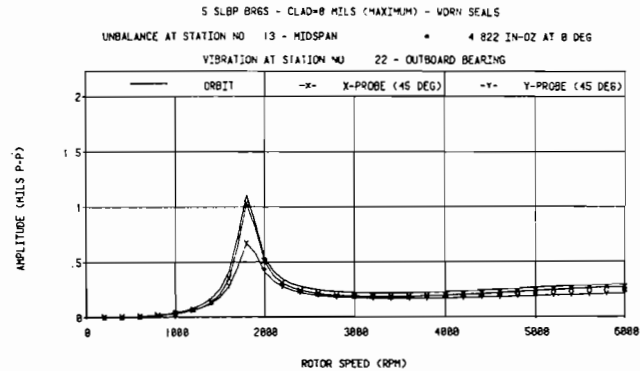

Figure 9. Calculated Unbalance Response at Outboard Bearing for API Unbalance at Midspan (Maximum (Worn) Seal Clearances, Maximum Bearing Clearance).
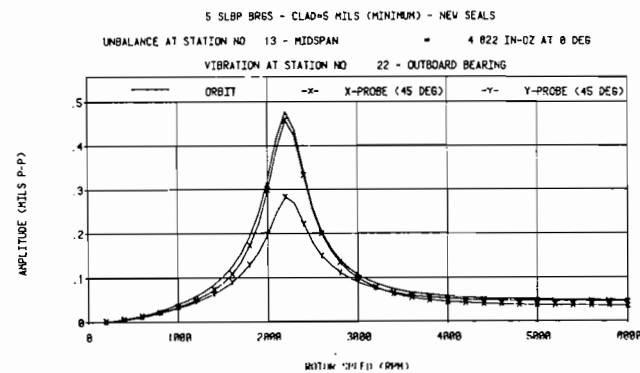

Figure 10. Calculated Unbalance Response at Outboard Bearing for API Unbalance at Midspan (Minimum (New) Seal Clearances, Minimum Bearing Clearance).
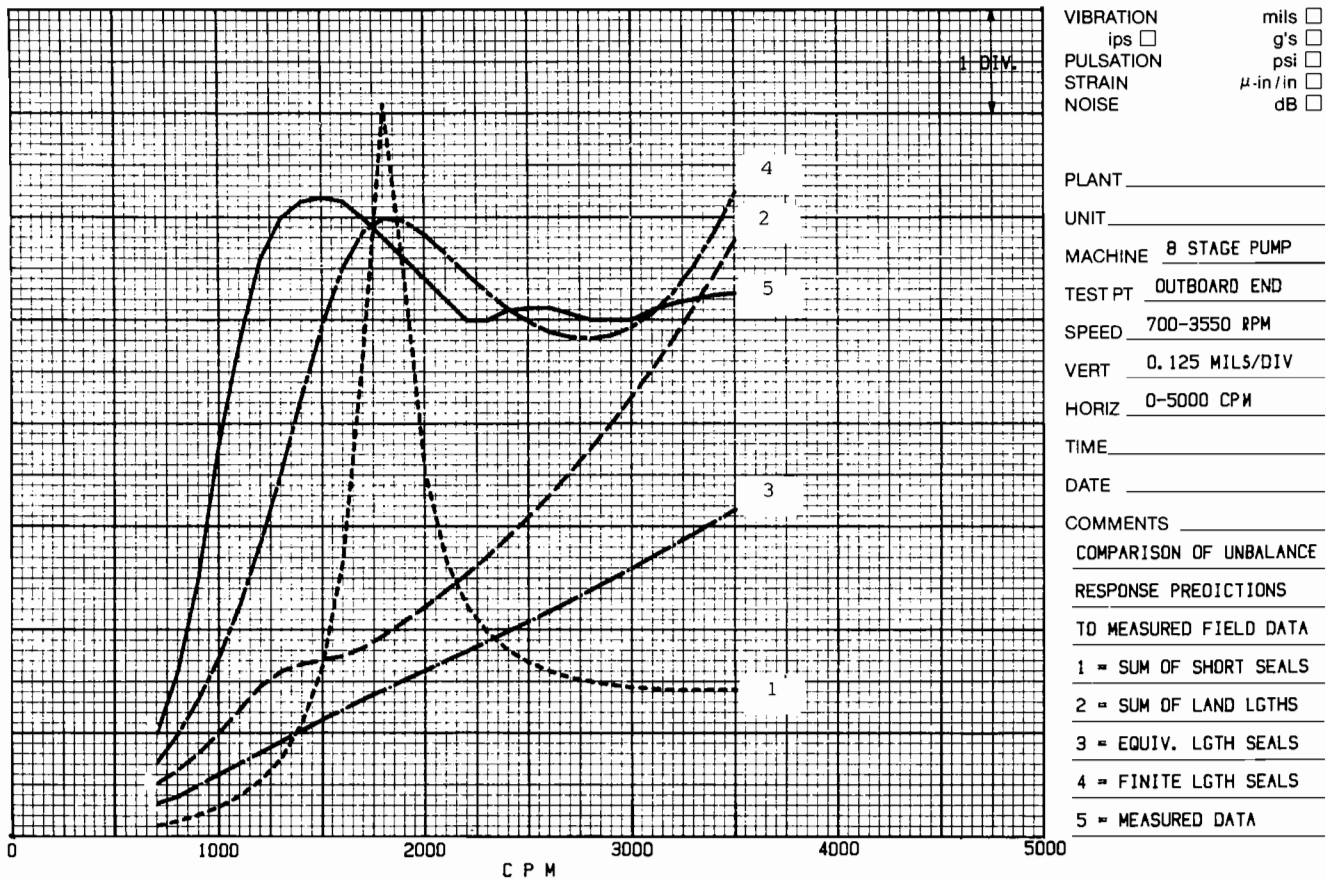
Figure 11. Comparison of Unbalance Response Predictions to Measured Field Data.

To illustrate the effects of calculating the seal stiffness and damping coefficients by the various methods, unbalance response predictions were made for each of the four seal assumptions. For these calculations, maximum bearing clearances and the design seal clearances were used. The unbalance was located at the rotor midspan. The unbalance response plots for each of the four calculation methods were overlaid with the measured vibration data from the test stand and are shown in Figure 11. This shows that Method 4 has the best correlation with the measured data. Method 1 predicts the same frequency as Method 4; however, the damping appears to be significantly underestimated. Method 2 shows a slight inflection near 1400 cpm with the amplitude being substantially lower than the measured amplitude. Method 3 overestimates the Lomakin effect and predicts the critical speeds to be above the running speed.

Based on these results, it appears that the Childs-Kim finite length method, currently under development, provides results most consistent with measured data. The "shape" of the response curve using the Childs-Kim seal values compares much more favorably than any of the other methods, indicating that the damping contribution of the seals is realistic. It is hoped that additional correlations between calculations, tests, and actual field data will be published as they become available.

CONCLUSIONS

The accurate calculation of pump critical speeds and stability requires accurate estimates of the stiffness and damping characteristics of grooved seals. Several methods that have been used to calculate the dynamic properties of seals were reviewed. Depending on the methods used to calculate the seal properties, substantial differences in the location of calculated pump critical speeds can occur, and in some cases, the critical speed may be predicted not to exist at any speed.

The seal properties calculated by the current Childs-Kim method appear to result in predicted rotor unbalance response which agrees most favorably with actual measured response. However, this is the only comparison made to date by the authors using this method.

It is apparent that a continuing effort toward the understanding of seals, including measurement and modelling techniques, is required before the unbalance response characteristics of pumps can be predicted accurately.

REFERENCES

1. Childs, D. W., "The Space Shuttle Main Engine High Pressure Fuel Turbopump Rotordynamic Instability Problem," ASME Transactions, Journal of Engineering for Power, pp. 48-57 (January 1978).

2. Gopalakrishnan, S., et.al., "Critical Speed in Centrifugal Pumps," ASME Paper 82-GT-277 (1982).

3. Childs, D. W., "Dynamic Analysis of Turbulent Annular Seals Based on Hirs' Lubrication Equation," ASME Transaction, Journal of Lubrication Technology, 105, pp. 429-436 (July 1983).

4. Childs, D. W., "Finite Length Solution for Rotordynamic Coefficients of Turbulent Annular Seals," ASME Transactions, Journal of Lubrication Technology, 105, pp. 437-445 (July 1983).

5. Childs, D. W. and Kim, C. H., "Analysis and Testing for Rotordynamic Coefficients of Turbulent Annular Seals with Different, Directionally-Homogeneous Surface-Roughness Treatment for Rotor and Stator Elements," ASME paper, ASME-ASLE Joint Lubrication Conference (October 1984).

6. Black, H. F., "Effects of Hydraulic Forces in Annular Pressure Seals on the Vibrations of Centrifugal Pump Rotors," Journal of Mechanical Engineering Science, *11, (2)* (1969).

7. Black, H. F. and Cochrane, E. A., "Leakage and Hybrid Bearing Properties of Serrated Seals in Centrifugal Pumps," 6th International Conference on Fluid Sealing, Munich, German Federal Republic, Paper G5 (1983).

8. Childs, D. W. and Moyer, D. S., "Vibration Characteristics of the HPOTP of the SSME," ASME Paper 84-GT-31 (1984).

9. Black, H. F. and Jenssen, D. N., "Dynamic Hybrid Properties of Annular Pressure Seals," ASME Paper 71-WA/FF-38 (1971).

10. Von Pragenau, G. L., "Damping Seals for Turbomachinery," NASA TP-1987 (March 1982).

11. Allaire, P., Lee, C., and Farris, R., "Turbulent Flow in Seals: Load Capacity and Dynamic Coefficients," University of Virginia Report No. UVA/464761/ME76/139 (December 1976).

12. Bolleter, U., Frei, A., and Florjancic, D., "Predicting and Improving the Dynamic Behavior of Multistage High Performance Pumps," *Proceedings of the First International Pump Symposium,* Texas A&M University, College Station, Texas, pp. 1-8 (May 1984).

13. Wachel, J. C., "Rotor Response and Sensitivity," Proceedings Vibration Institute Machinery Vibration Monitoring and Analysis, Houston, Texas, pp. 1-12 (April 1983).